BABAR Analysis Document # 2236, Version 6

Search for $\overline{B} \to \Lambda_c^+ X \ell^- \overline{\nu}_\ell$ Decays in Events Tagged by a Fully Reconstructed B Meson

J. P. Lees,[1] V. Poireau,[1] V. Tisserand,[1] J. Garra Tico,[2] E. Grauges,[2] M. Martinelli[ab],[3] D. A. Milanes[a],[3] A. Palano[ab],[3] M. Pappagallo[ab],[3] G. Eigen,[4] B. Stugu,[4] L. Sun,[4] D. N. Brown,[5] L. T. Kerth,[5] Yu. G. Kolomensky,[5] G. Lynch,[5] H. Koch,[6] T. Schroeder,[6] D. J. Asgeirsson,[7] C. Hearty,[7] T. S. Mattison,[7] J. A. McKenna,[7] A. Khan,[8] V. E. Blinov,[9] A. R. Buzykaev,[9] V. P. Druzhinin,[9] V. B. Golubev,[9] E. A. Kravchenko,[9] A. P. Onuchin,[9] S. I. Serednyakov,[9] Yu. I. Skovpen,[9] E. P. Solodov,[9] K. Yu. Todyshev,[9] A. N. Yushkov,[9] M. Bondioli,[10] D. Kirkby,[10] A. J. Lankford,[10] M. Mandelkern,[10] D. P. Stoker,[10] H. Atmacan,[11] J. W. Gary,[11] F. Liu,[11] O. Long,[11] G. M. Vitug,[11] C. Campagnari,[12] T. M. Hong,[12] D. Kovalskyi,[12] J. D. Richman,[12] C. A. West,[12] A. M. Eisner,[13] J. Kroseberg,[13] W. S. Lockman,[13] A. J. Martinez,[13] T. Schalk,[13] B. A. Schumm,[13] A. Seiden,[13] C. H. Cheng,[14] D. A. Doll,[14] B. Echenard,[14] K. T. Flood,[14] D. G. Hitlin,[14] P. Ongmongkolkul,[14] F. C. Porter,[14] A. Y. Rakitin,[14] R. Andreassen,[15] M. S. Dubrovin,[15] Z. Huard,[15] B. T. Meadows,[15] M. D. Sokoloff,[15] P. C. Bloom,[16] W. T. Ford,[16] A. Gaz,[16] M. Nagel,[16] U. Nauenberg,[16] J. G. Smith,[16] S. R. Wagner,[16] R. Ayad,[17,*] W. H. Toki,[17] B. Spaan,[18] M. J. Kobel,[19] K. R. Schubert,[19] R. Schwierz,[19] D. Bernard,[20] M. Verderi,[20] P. J. Clark,[21] S. Playfer,[21] D. Bettoni[a],[22] C. Bozzi[a],[22] R. Calabrese[ab],[22] G. Cibinetto[ab],[22] E. Fioravanti[ab],[22] I. Garzia[ab],[22] E. Luppi[ab],[22] M. Munerato[ab],[22] M. Negrini[ab],[22] L. Piemontese[a],[22] R. Baldini-Ferroli,[23] A. Calcaterra,[23] R. de Sangro,[23] G. Finocchiaro,[23] M. Nicolaci,[23] P. Patteri,[23] I. M. Peruzzi,[23,†] M. Piccolo,[23] M. Rama,[23] A. Zallo,[23] R. Contri[ab],[24] E. Guido[ab],[24] M. Lo Vetere[ab],[24] M. R. Monge[ab],[24] S. Passaggio[a],[24] C. Patrignani[ab],[24] E. Robutti[a],[24] B. Bhuyan,[25] V. Prasad,[25] C. L. Lee,[26] M. Morii,[26] A. J. Edwards,[27] A. Adametz,[28] J. Marks,[28] U. Uwer,[28] F. U. Bernlochner,[29] M. Ebert,[29] H. M. Lacker,[29] T. Lueck,[29] P. D. Dauncey,[30] M. Tibbetts,[30] P. K. Behera,[31] U. Mallik,[31] C. Chen,[32] J. Cochran,[32] W. T. Meyer,[32] S. Prell,[32] E. I. Rosenberg,[32] A. E. Rubin,[32] A. V. Gritsan,[33] Z. J. Guo,[33] N. Arnaud,[34] M. Davier,[34] G. Grosdidier,[34] F. Le Diberder,[34] A. M. Lutz,[34] B. Malaescu,[34] P. Roudeau,[34] M. H. Schune,[34] A. Stocchi,[34] G. Wormser,[34] D. J. Lange,[35] D. M. Wright,[35] I. Bingham,[36] C. A. Chavez,[36] J. P. Coleman,[36] J. R. Fry,[36] E. Gabathuler,[36] D. E. Hutchcroft,[36] D. J. Payne,[36] C. Touramanis,[36] A. J. Bevan,[37] F. Di Lodovico,[37] R. Sacco,[37] M. Sigamani,[37] G. Cowan,[38] S. Paramesvaran,[38] D. N. Brown,[39] C. L. Davis,[39] A. G. Denig,[40] M. Fritsch,[40] W. Gradl,[40] A. Hafner,[40] E. Prencipe,[40] K. E. Alwyn,[41] D. Bailey,[41] R. J. Barlow,[41] G. Jackson,[41] G. D. Lafferty,[41] R. Cenci,[42] B. Hamilton,[42] A. Jawahery,[42] D. A. Roberts,[42] G. Simi,[42] C. Dallapiccola,[43] R. Cowan,[44] D. Dujmic,[44] G. Sciolla,[44] D. Lindemann,[45] P. M. Patel,[45] S. H. Robertson,[45] M. Schram,[45] P. Biassoni[ab],[46] A. Lazzaro[ab],[46] V. Lombardo[a],[46] N. Neri[ab],[46] F. Palombo[ab],[46] S. Stracka[ab],[46] L. Cremaldi,[47] R. Godang,[47,‡] R. Kroeger,[47] P. Sonnek,[47] D. J. Summers,[47] X. Nguyen,[48] P. Taras,[48] G. De Nardo[ab],[49] D. Monorchio[ab],[49] G. Onorato[ab],[49] C. Sciacca[ab],[49] G. Raven,[50] H. L. Snoek,[50] C. P. Jessop,[51] K. J. Knoepfel,[51] J. M. LoSecco,[51] W. F. Wang,[51] K. Honscheid,[52] R. Kass,[52] J. Brau,[53] R. Frey,[53] N. B. Sinev,[53] D. Strom,[53] E. Torrence,[53] E. Feltresi[ab],[54] N. Gagliardi[ab],[54] M. Margoni[ab],[54] M. Morandin[a],[54] M. Posocco[a],[54] M. Rotondo[a],[54] F. Simonetto[ab],[54] R. Stroili[ab],[54] E. Ben-Haim,[55] M. Bomben,[55] G. R. Bonneaud,[55] H. Briand,[55] G. Calderini,[55] J. Chauveau,[55] O. Hamon,[55] Ph. Leruste,[55] G. Marchiori,[55] J. Ocariz,[55] S. Sitt,[55] M. Biasini[ab],[56] E. Manoni[ab],[56] S. Pacetti[ab],[56] A. Rossi[ab],[56] C. Angelini[ab],[57] G. Batignani[ab],[57] S. Bettarini[ab],[57] M. Carpinelli[ab],[57,§] G. Casarosa[ab],[57] A. Cervelli[ab],[57] F. Forti[ab],[57] M. A. Giorgi[ab],[57] A. Lusiani[ac],[57] B. Oberhof[ab],[57] E. Paoloni[ab],[57] A. Perez[a],[57] G. Rizzo[ab],[57] J. J. Walsh[a],[57] D. Lopes Pegna,[58] C. Lu,[58] J. Olsen,[58] A. J. S. Smith,[58] A. V. Telnov,[58] F. Anulli[a],[59] G. Cavoto[a],[59] R. Faccini[ab],[59] F. Ferrarotto[a],[59] F. Ferroni[ab],[59] M. Gaspero[ab],[59] L. Li Gioi[a],[59] M. A. Mazzoni[a],[59] G. Piredda[a],[59] C. Bünger,[60] O. Grünberg,[60] T. Hartmann,[60] T. Leddig,[60] H. Schröder,[60] R. Waldi,[60] T. Adye,[61] E. O. Olaiya,[61] F. F. Wilson,[61] S. Emery,[62] G. Hamel de Monchenault,[62] G. Vasseur,[62] Ch. Yèche,[62] D. Aston,[63] D. J. Bard,[63] R. Bartoldus,[63] C. Cartaro,[63] M. R. Convery,[63] J. Dorfan,[63] G. P. Dubois-Felsmann,[63] W. Dunwoodie,[63] R. C. Field,[63] M. Franco Sevilla,[63] B. G. Fulsom,[63] A. M. Gabareen,[63] M. T. Graham,[63] P. Grenier,[63] C. Hast,[63] W. R. Innes,[63] M. H. Kelsey,[63] H. Kim,[63] P. Kim,[63] M. L. Kocian,[63] D. W. G. S. Leith,[63] P. Lewis,[63] S. Li,[63] B. Lindquist,[63] S. Luitz,[63] V. Luth,[63] H. L. Lynch,[63] D. B. MacFarlane,[63] D. R. Muller,[63] H. Neal,[63] S. Nelson,[63] I. Ofte,[63] M. Perl,[63] T. Pulliam,[63] B. N. Ratcliff,[63] A. Roodman,[63] A. A. Salnikov,[63] V. Santoro,[63] R. H. Schindler,[63] A. Snyder,[63] D. Su,[63] M. K. Sullivan,[63] J. Va'vra,[63] A. P. Wagner,[63] M. Weaver,[63] W. J. Wisniewski,[63] M. Wittgen,[63] D. H. Wright,[63] H. W. Wulsin,[63] A. K. Yarritu,[63] C. C. Young,[63] V. Ziegler,[63] W. Park,[64] M. V. Purohit,[64] R. M. White,[64] J. R. Wilson,[64] A. Randle-Conde,[65] S. J. Sekula,[65] M. Bellis,[66] J. F. Benitez,[66] P. R. Burchat,[66] T. S. Miyashita,[66] M. S. Alam,[67] J. A. Ernst,[67] R. Gorodeisky,[68] N. Guttman,[68] D. R. Peimer,[68] A. Soffer,[68] P. Lund,[69] S. M. Spanier,[69] R. Eckmann,[70] J. L. Ritchie,[70] A. M. Ruland,[70] C. J. Schilling,[70] R. F. Schwitters,[70] B. C. Wray,[70] J. M. Izen,[71] X. C. Lou,[71] F. Bianchi[ab],[72] D. Gamba[ab],[72] L. Lanceri[ab],[73] L. Vitale[ab],[73] F. Martinez-Vidal,[74] A. Oyanguren,[74] H. Ahmed,[75] J. Albert,[75] Sw. Banerjee,[75] H. H. F. Choi,[75] G. J. King,[75] R. Kowalewski,[75] M. J. Lewczuk,[75] C. Lindsay,[75] I. M. Nugent,[75] J. M. Roney,[75] R. J. Sobie,[75] T. J. Gershon,[76] P. F. Harrison,[76]

T. E. Latham,[76] E. M. T. Puccio,[76] H. R. Band,[77] S. Dasu,[77] Y. Pan,[77] R. Prepost,[77] C. O. Vuosalo,[77] and S. L. Wu[77]
(The *BABAR* Collaboration)

[1]*Laboratoire d'Annecy-le-Vieux de Physique des Particules (LAPP), Université de Savoie, CNRS/IN2P3, F-74941 Annecy-Le-Vieux, France*
[2]*Universitat de Barcelona, Facultat de Fisica, Departament ECM, E-08028 Barcelona, Spain*
[3]*INFN Sezione di Bari[a]; Dipartimento di Fisica, Università di Bari[b], I-70126 Bari, Italy*
[4]*University of Bergen, Institute of Physics, N-5007 Bergen, Norway*
[5]*Lawrence Berkeley National Laboratory and University of California, Berkeley, California 94720, USA*
[6]*Ruhr Universität Bochum, Institut für Experimentalphysik 1, D-44780 Bochum, Germany*
[7]*University of British Columbia, Vancouver, British Columbia, Canada V6T 1Z1*
[8]*Brunel University, Uxbridge, Middlesex UB8 3PH, United Kingdom*
[9]*Budker Institute of Nuclear Physics, Novosibirsk 630090, Russia*
[10]*University of California at Irvine, Irvine, California 92697, USA*
[11]*University of California at Riverside, Riverside, California 92521, USA*
[12]*University of California at Santa Barbara, Santa Barbara, California 93106, USA*
[13]*University of California at Santa Cruz, Institute for Particle Physics, Santa Cruz, California 95064, USA*
[14]*California Institute of Technology, Pasadena, California 91125, USA*
[15]*University of Cincinnati, Cincinnati, Ohio 45221, USA*
[16]*University of Colorado, Boulder, Colorado 80309, USA*
[17]*Colorado State University, Fort Collins, Colorado 80523, USA*
[18]*Technische Universität Dortmund, Fakultät Physik, D-44221 Dortmund, Germany*
[19]*Technische Universität Dresden, Institut für Kern- und Teilchenphysik, D-01062 Dresden, Germany*
[20]*Laboratoire Leprince-Ringuet, Ecole Polytechnique, CNRS/IN2P3, F-91128 Palaiseau, France*
[21]*University of Edinburgh, Edinburgh EH9 3JZ, United Kingdom*
[22]*INFN Sezione di Ferrara[a]; Dipartimento di Fisica, Università di Ferrara[b], I-44100 Ferrara, Italy*
[23]*INFN Laboratori Nazionali di Frascati, I-00044 Frascati, Italy*
[24]*INFN Sezione di Genova[a]; Dipartimento di Fisica, Università di Genova[b], I-16146 Genova, Italy*
[25]*Indian Institute of Technology Guwahati, Guwahati, Assam, 781 039, India*
[26]*Harvard University, Cambridge, Massachusetts 02138, USA*
[27]*Harvey Mudd College, Claremont, California 91711*
[28]*Universität Heidelberg, Physikalisches Institut, Philosophenweg 12, D-69120 Heidelberg, Germany*
[29]*Humboldt-Universität zu Berlin, Institut für Physik, Newtonstr. 15, D-12489 Berlin, Germany*
[30]*Imperial College London, London, SW7 2AZ, United Kingdom*
[31]*University of Iowa, Iowa City, Iowa 52242, USA*
[32]*Iowa State University, Ames, Iowa 50011-3160, USA*
[33]*Johns Hopkins University, Baltimore, Maryland 21218, USA*
[34]*Laboratoire de l'Accélérateur Linéaire, IN2P3/CNRS et Université Paris-Sud 11, Centre Scientifique d'Orsay, B. P. 34, F-91898 Orsay Cedex, France*
[35]*Lawrence Livermore National Laboratory, Livermore, California 94550, USA*
[36]*University of Liverpool, Liverpool L69 7ZE, United Kingdom*
[37]*Queen Mary, University of London, London, E1 4NS, United Kingdom*
[38]*University of London, Royal Holloway and Bedford New College, Egham, Surrey TW20 0EX, United Kingdom*
[39]*University of Louisville, Louisville, Kentucky 40292, USA*
[40]*Johannes Gutenberg-Universität Mainz, Institut für Kernphysik, D-55099 Mainz, Germany*
[41]*University of Manchester, Manchester M13 9PL, United Kingdom*
[42]*University of Maryland, College Park, Maryland 20742, USA*
[43]*University of Massachusetts, Amherst, Massachusetts 01003, USA*
[44]*Massachusetts Institute of Technology, Laboratory for Nuclear Science, Cambridge, Massachusetts 02139, USA*
[45]*McGill University, Montréal, Québec, Canada H3A 2T8*
[46]*INFN Sezione di Milano[a]; Dipartimento di Fisica, Università di Milano[b], I-20133 Milano, Italy*
[47]*University of Mississippi, University, Mississippi 38677, USA*
[48]*Université de Montréal, Physique des Particules, Montréal, Québec, Canada H3C 3J7*
[49]*INFN Sezione di Napoli[a]; Dipartimento di Scienze Fisiche, Università di Napoli Federico II[b], I-80126 Napoli, Italy*
[50]*NIKHEF, National Institute for Nuclear Physics and High Energy Physics, NL-1009 DB Amsterdam, The Netherlands*
[51]*University of Notre Dame, Notre Dame, Indiana 46556, USA*
[52]*Ohio State University, Columbus, Ohio 43210, USA*
[53]*University of Oregon, Eugene, Oregon 97403, USA*
[54]*INFN Sezione di Padova[a]; Dipartimento di Fisica, Università di Padova[b], I-35131 Padova, Italy*
[55]*Laboratoire de Physique Nucléaire et de Hautes Energies, IN2P3/CNRS, Université Pierre et Marie Curie-Paris6, Université Denis Diderot-Paris7, F-75252 Paris, France*
[56]*INFN Sezione di Perugia[a]; Dipartimento di Fisica, Università di Perugia[b], I-06100 Perugia, Italy*

[57]INFN Sezione di Pisa[a]; Dipartimento di Fisica, Università di Pisa[b]; Scuola Normale Superiore di Pisa[c], I-56127 Pisa, Italy
[58]Princeton University, Princeton, New Jersey 08544, USA
[59]INFN Sezione di Roma[a]; Dipartimento di Fisica, Università di Roma La Sapienza[b], I-00185 Roma, Italy
[60]Universität Rostock, D-18051 Rostock, Germany
[61]Rutherford Appleton Laboratory, Chilton, Didcot, Oxon, OX11 0QX, United Kingdom
[62]CEA, Irfu, SPP, Centre de Saclay, F-91191 Gif-sur-Yvette, France
[63]SLAC National Accelerator Laboratory, Stanford, California 94309 USA
[64]University of South Carolina, Columbia, South Carolina 29208, USA
[65]Southern Methodist University, Dallas, Texas 75275, USA
[66]Stanford University, Stanford, California 94305-4060, USA
[67]State University of New York, Albany, New York 12222, USA
[68]Tel Aviv University, School of Physics and Astronomy, Tel Aviv, 69978, Israel
[69]University of Tennessee, Knoxville, Tennessee 37996, USA
[70]University of Texas at Austin, Austin, Texas 78712, USA
[71]University of Texas at Dallas, Richardson, Texas 75083, USA
[72]INFN Sezione di Torino[a]; Dipartimento di Fisica Sperimentale, Università di Torino[b], I-10125 Torino, Italy
[73]INFN Sezione di Trieste[a]; Dipartimento di Fisica, Università di Trieste[b], I-34127 Trieste, Italy
[74]IFIC, Universitat de Valencia-CSIC, E-46071 Valencia, Spain
[75]University of Victoria, Victoria, British Columbia, Canada V8W 3P6
[76]Department of Physics, University of Warwick, Coventry CV4 7AL, United Kingdom
[77]University of Wisconsin, Madison, Wisconsin 53706, USA

(Dated: May 4, 2011)

We present a search for semi-leptonic B decays to the charmed baryon Λ_c^+ based on 420 fb^{-1} of data collected at the $\Upsilon(4S)$ resonance with the *BABAR* detector at the PEP-II e^+e^- storage rings. By fully reconstructing the recoiling B in a hadronic decay mode, we reduce non-B backgrounds, and determine the flavor of the signal B, modulo the effect of B^0 mixing, which is corrected for statistically. We measure the relative branching fraction $\mathcal{B}(\overline{B} \to \Lambda_c^+ X \ell^- \overline{\nu}_\ell)/\mathcal{B}(\overline{B} \to \Lambda_c^+ X) = (1.7 \pm 1.0_{\rm stat.} \pm 0.6_{\rm syst.})\%$, averaged over $\ell = e$ and μ, corresponding to a 90% confidence level upper limit of $\mathcal{B}(\overline{B} \to \Lambda_c^+ X \ell^- \overline{\nu}_\ell)/\mathcal{B}(\overline{B} \to \Lambda_c^+ X) < 3.5\%$.

PACS numbers: 13.20He, 12.38.Qk, 14.40Nd

Decays of B mesons to charmed baryons are not as well understood as B decays to charmed mesons. In particular, there is limited knowledge, both theoretical and experimental, about semi-leptonic B decays to the Λ_c^+ charmed baryon. If B decays to charmed baryons are dominated by external W emission (Fig. 1a), as is the case for B decays to charmed mesons, and final-state hadronic interactions are small, the semi-leptonic fraction of these decays should be roughly the same [1]:

$$\frac{\mathcal{B}(\overline{B} \to \Lambda_c^+ X \ell^- \overline{\nu}_\ell)}{\mathcal{B}(\overline{B} \to \Lambda_c^+ X)} \sim \frac{\mathcal{B}(\overline{B} \to D X \ell^- \overline{\nu}_\ell)}{\mathcal{B}(\overline{B} \to D X)} \qquad (1)$$

where $\ell = e$ or μ. The semi-leptonic fraction of B decays to charmed mesons is currently measured to be about 10% [2]. A significantly smaller semi-leptonic ratio for B decays to charmed baryons would be evidence for a sizable internal W emission amplitude in baryonic B decay (Fig. 1b), or of large final state interactions.

About 90% of the measured inclusive semi-leptonic $\overline{B} \to X_c \ell^- \overline{\nu}_\ell$ branching fraction into charmed final states can be accounted for by summing the branching fractions from exclusive $\overline{B} \to D^{(*)}(\pi)\ell^- \overline{\nu}_\ell$ decays [3]. Semi-leptonic B decays to charmed baryons could account for some of the remaining difference.

A previous search for semi-leptonic B decays into charmed baryons by the CLEO collaboration [4] resulted in an upper limit on the ratio $\mathcal{B}(\overline{B} \to \Lambda_c^+ X e^- \overline{\nu}_e)/\mathcal{B}(\overline{B} \to \Lambda_c^+/\overline{\Lambda}_c^- X) < 5\%$ at the 90% confidence level. By using $\mathcal{B}(\overline{B} \to \Lambda_c^+/\overline{\Lambda}_c^- X) = 0.045 \pm 0.004 \pm 0.012$ and $\mathcal{B}(\overline{B} \to \overline{\Lambda}_c^- X)/\mathcal{B}(\overline{B} \to \Lambda_c^+ X) = 0.19 \pm 0.13 \pm 0.04$ [2], and assuming lepton universality, this result implies a semi-leptonic fraction limit $\mathcal{B}(\overline{B} \to \Lambda_c^+ X \ell^- \overline{\nu}_\ell)/\mathcal{B}(\overline{B} \to \Lambda_c^+ X) < 6\%$ at 90% confidence level.

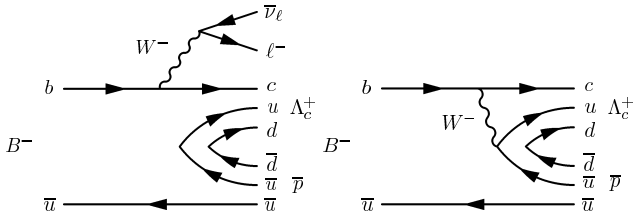

FIG. 1: Feynman diagrams for charged B decays into a charmed baryon through external W emission (a) and internal W emission (b).

In this paper, we present a search for semi-leptonic B decays to Λ_c^+ using data collected with the *BABAR* detector at the PEP-II asymmetric-energy e^+e^- storage rings at SLAC. The data consist of a total of 420 fb^{-1} recorded at the $\Upsilon(4S)$ resonance, corresponding to approximately 460 million $B\overline{B}$ pairs. The *BABAR* detector is described in detail elsewhere [5]. Charged-particle trajectories are measured by a 5-layer double-sided silicon vertex tracker and a 40-layer drift chamber, both operating in a 1.5-T magnetic field. Charged-particle identification is provided by the average energy loss (dE/dx) in the tracking devices and by an internally reflect-

ing ring-imaging Cherenkov detector. Photons are detected by a CsI(Tl) electromagnetic calorimeter. Muons are identified by the instrumented magnetic-flux return. A detailed GEANT4-based Monte Carlo simulation [6] of $B\overline{B}$ and continuum events (light quarks and τ pairs) is used to study the detector response, its acceptance, and to test the analysis techniques.

We search for semi-leptonic $\overline{B} \to \Lambda_c^+ X \ell^- \overline{\nu}_\ell$ decays with $\ell = e$ or μ in events pre-selected to contain a candidate B reconstructed in a fully hadronic decay mode ($B_{\rm tag}$), as described later in the text. We select signal candidates in these events by looking for candidate leptons and fully reconstructed Λ_c^+ decays. We then refine our selection of $B_{\rm tag}$, and make a final signal extraction based on the selected $B_{\rm tag}$ and Λ_c^+ kinematic properties. We also select candidate $\overline{B} \to \Lambda_c^+ X$ events, starting with the same sample and using similar techniques and cuts, but without requiring an identified lepton candidate.

Selection cuts are optimized using Monte Carlo simulation of signal and background processes. Because little is known about $\overline{B} \to \Lambda_c^+ X \ell^- \overline{\nu}_\ell$ decay, we use an ad-hoc signal model which can be tuned to cover a large range of possible kinematics of the final state particles. In our model the B decays semi-leptonically into an intermediate massive particle Y, $\overline{B} \to Y \ell^- \overline{\nu}_\ell$, with a kinematic distribution according to phase space [8]. The Y subsequently decays into a Λ_c^+, an anti-nucleon (anti-proton or anti-neutron), and n_1 (n_2) charged (neutral) pions, again assuming phase space distributions, with isospin symmetry required in the final state. The free parameters in the model (the mass m_Y and width Γ_Y of the pseudo-particle Y, and n_1 and n_2) are tuned to reproduce the lepton and charmed hadron momentum spectra predicted by the $\overline{B} \to D^{(*)} \pi \ell \overline{\nu}_\ell$ model of Goity and Roberts [9], after accounting for the phase space limits implied by the large baryon masses. We choose $m_Y = 4.5$ GeV/c^2, $\Gamma_Y = 0.2$ GeV/c^2, and $n_1 + n_2 \leq 6$.

We reconstruct $B_{\rm tag}$ decays of the type $B \to \overline{D} Y'$, where Y' represents a collection of hadrons with a total charge of ± 1, composed of $n_1' \pi^\pm + n_2' K^\pm + n_3' K_S^0 + n_4' \pi^0$, where $n_1' + n_2' \leq 5$, $n_3' \leq 2$, and $n_4' \leq 2$. Using D^0 (D^+) and D^{*0} (D^{*+}) as seeds for B^- ($\overline{B}^0$) decays, we reconstruct about 1000 complete B decay chains [7]. The kinematic consistency of a $B_{\rm tag}$ candidate with a B meson decay is evaluated using two variables: the beam-energy substituted mass $m_{ES} \equiv \sqrt{s/4 - |p_B^*|^2}$, and the energy difference $\Delta E \equiv E_B^* - \sqrt{s}/2$. Here $\sqrt{s}$ is the total center of mass (CM) energy, and p_B^* and E_B^* denote the momentum and energy of the $B_{\rm tag}$ candidate in the CM frame. For correctly identified $B_{\rm tag}$ decays, the m_{ES} distribution peaks at the B meson mass, with a resolution of about 2.5 MeV/c^2, while ΔE is consistent with zero, with a resolution of about 18 MeV. We select $B_{\rm tag}$ candidates in the signal region defined as 5.27 GeV/$c^2 < m_{ES} <$ 5.29 GeV/c^2, with a ΔE within 4σ of zero. For each $B_{\rm tag}$ decay chain, the *a priori* purity $\mathcal{P}$ is estimated using Monte Carlo simulation as the ratio of signal over background events. This selection has an estimated efficiency of 0.2 to 0.3% per B meson.

We identify electron candidates based on the combined information of the measured momentum and energy loss in the SVT and DCH, the angle of Cherenkov radiation in the DRC, and the energy deposition and shower shape in the EMC. We correct for bremsstrahlung of electrons by combining detected photons which are emitted close to the electron direction. We select muon candidates through the detector information from the IFR, in addition to the variables used in the electron identification. Furthermore, we require lepton candidates to have a momentum in the CM frame $p_\ell^* > 0.35$ GeV/c, and with a point of closest approach to the interaction point in the transverse plane of less than 0.1 cm. The p_ℓ^* cut value is motivated by the large mass of the Λ_c^+ and the assumption of another baryon in the decay due to baryon number conservation, which greatly restricts the available kinetic energy. We identify photon conversions and π^0 Dalitz decays using a dedicated algorithm based on the vertex and kinematic properties of two opposite charge tracks, and eliminate electron candidates coming from these.

Candidate Λ_c^+ baryons are reconstructed in the $pK^-\pi^+$, pK_S^0, $pK_S^0\pi^+\pi^-$, $\Lambda\pi^+$, $\Lambda\pi^+\pi^+\pi^-$ modes. K_S^0 candidates are reconstructed in the $\pi^+\pi^-$ decay mode, Λ candidates in the $p\pi^-$ decay mode. Only Λ_c candidates with opposite charge as the lepton candidate are considered. Charged particles daughters of the Λ_c^+ candidate are fit to a vertex tree [10], with K_S^0 and Λ masses constrained to their measured values [2], and the Λ_c^+ origin constrained to the known average luminous position within its size and measured errors. In events with multiple Λ_c^+ and/or ℓ candidates, the candidates are fit to a common vertex, and the Λ_c^+-ℓ^- pair with the highest vertex fit probability is selected.

We select final $B_{\rm tag}$ candidates by first removing those whose daughter particles are based on tracks already used to reconstruct the signal-side Λ_c^+ or lepton, and those charged $B_{\rm tag}$ whose flavor is inconsistent with $\overline{B} \to \Lambda_c^+ X \ell^- \overline{\nu}_\ell$ on the signal side, given the measured Λ_c charge. We account for mixing effects by appropriately weighting B^0 and $\overline{B}^0$ tags according to the Λ_c charge, as described in Ref. [11]. In events with multiple $B_{\rm tag}$ candidates, we select the one decaying in the highest *a priori* purity $\mathcal{P}$ mode. When multiple candidates in the same event have the same $B_{\rm tag}$ mode, we select the one with the smallest $|\Delta E|$ value.

We reconstruct the missing momentum $P_{\rm miss}$ in selected events by subtracting the CM three-momentum of the $B_{\rm tag}$, the Λ_c and ℓ candidates, plus any additional well-measured charged track or neutral cluster, from the null vector. We require $|P_{\rm miss}| > 0.2$ GeV/c, which removes background from hadronic $\overline{B} \to \Lambda_c^+ X$ decays in which all the particles in the X system have been reconstructed and one hadron is misidentified as a lepton. We compute the total charge of selected events by adding the charges of all particles used in the $P_{\rm miss}$ calculation, and require this to be zero. This reduces the combinatorial background in the $B_{\rm tag}$ reconstruction from missing particles.

We determine the B semi-leptonic signal yield with a simultaneous one-dimensional unbinned maximum likelihood fit to the Λ_c^+ invariant mass distribution in both the electron

and muon samples. Backgrounds can be divided according to whether they contain a Λ_c^+ candidate with a mass value in the signal region (peaking), and those that do not. Monte Carlo studies of generic $B\overline{B}$ and continuum events show that the peaking background comes mainly from hadronic $\overline{B} \to \Lambda_c^+ X$ decays, where the Λ_c^+ is correctly reconstructed, and the lepton candidate is either an electron from gamma conversions or π^0 Dalitz decays, or a hadron misidentified as a muon. We estimate $N_{\rm peak} = 3.6 \pm 0.7_{\rm stat.} \pm 0.7_{\rm syst.}$ and $N_{\rm peak} = 15.3 \pm 1.5_{\rm stat.} \pm 1.4_{\rm syst.}$ peaking background events for the electron and muon samples, respectively. The sources of systematic error are described in the following.

The Λ_c^+ invariant mass distribution is described as the sum of three probability density functions (PDFs) representing signal, peaking background, and combinatorial background. The functional forms of the PDFs are chosen based on simulation studies. The signal and peaking background contributions are modeled as Gaussians whose mean and width are fixed to the values obtained from a fit to the the Λ_c^+ mass spectrum in the $\overline{B} \to \Lambda_c^+ X$ data sample described below. The number of peaking background events is fixed to the Monte Carlo prediction. The combinatorial $B\overline{B}$ and continuum backgrounds are modeled as a first order polynomial, whose parameters are constrained by a fit to the Λ_c^+ invariant mass sidebands, defined as the mass ranges from $2.23 - 2.26$ and $2.31 - 2.34$ GeV/c^2. The fit to the Λ_c^+ invariant mass is shown in Fig. 2, projected separately for the electron and muon samples.

In order to reduce systematic uncertainties due to $B_{\rm tag}$ and Λ_c^+ reconstruction, the $\mathcal{B}(\overline{B} \to \Lambda_c^+ X \ell^- \overline{\nu}_\ell)$ branching fraction is measured relative to the inclusive $\mathcal{B}(\overline{B} \to \Lambda_c^+ X)$ branching fraction. To determine the inclusive yield, we start with the same $B_{\rm tag}$ sample used for the semi-leptonic selection. We reconstruct Λ_c^+ candidates as in the semi-leptonic case, choosing the candidate with the highest vertex probability in case of multiple candidates. We exclude $B_{\rm tag}$ candidates with daughter particles in common with the Λ_c^+ candidate, and resolve multiple $B_{\rm tag}$ candidates as in the semi-leptonic case.

We determine the $\overline{B} \to \Lambda_c^+ X$ signal yield with a one-dimensional unbinned maximum likelihood fit to the Λ_c^+ invariant mass distribution. That distribution is described as the sum of two PDFs representing signal and combinatorial background, described as a single Gaussian and a first order polynomial, respectively. All parameters of the signal Gaussian are left free in the fit. We obtain a Λ_c^+ mass value of 2.2853 ± 0.0003 GeV/c^2, consistent with the current world average [2], and a resolution of 4.0 ± 0.3 MeV/c^2, consistent with Monte Carlo expectations. The Λ_c^+ invariant mass distribution and the results of the inclusive fit are shown in Fig. 3.

We determine the relative branching fraction $\mathcal{B}(\overline{B} \to \Lambda_c^+ X \ell^- \overline{\nu}_\ell)/\mathcal{B}(\overline{B} \to \Lambda_c^+ X)$ as the ratio of the measured signal yields, after correcting for the reconstruction efficiency ratio:

$$\frac{\mathcal{B}(\overline{B} \to \Lambda_c^+ X \ell^- \overline{\nu}_\ell)}{\mathcal{B}(\overline{B} \to \Lambda_c^+ X)} = \left(\frac{N_{\rm semil}}{N_{\rm had}}\right)\left(\frac{\varepsilon_{\rm had}}{\varepsilon_{\rm semil}}\right). \qquad (2)$$

Here, $N_{\rm semil}$ ($N_{\rm had}$) is the number of $\overline{B} \to \Lambda_c^+ X$ signal events for the semi-leptonic (inclusive) mode, reported in Table I together with the corresponding reconstruction efficiencies ε estimated on signal Monte Carlo events.

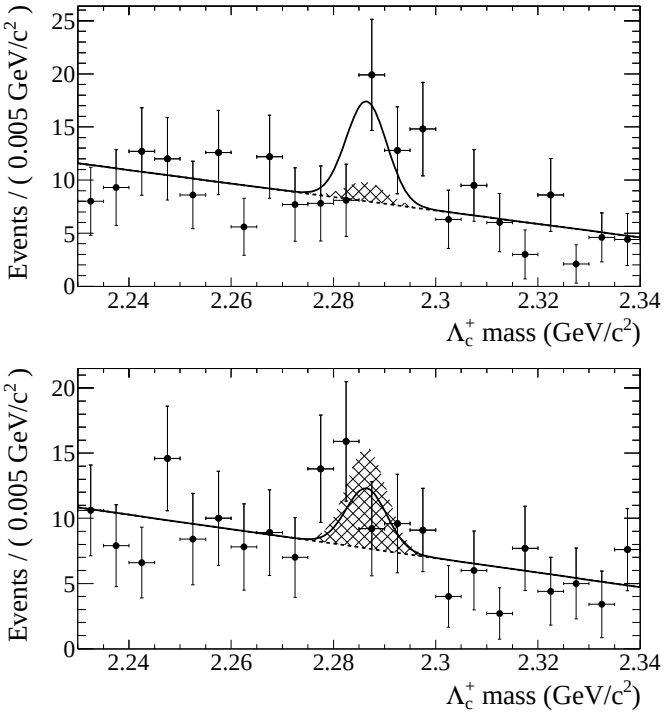

FIG. 2: Fit to the Λ_c^+ distribution for $\overline{B} \to \Lambda_c^+ X e^- \overline{\nu}_e$ (top) and $\overline{B} \to \Lambda_c^+ X \mu^- \overline{\nu}_\mu$ (bottom). The data are shown as points with error bars, the overall fit as a solid line, the peaking background contribution as a cross-hatched area, and the combinatorial $B\overline{B}$ and continuum background as a dashed line.

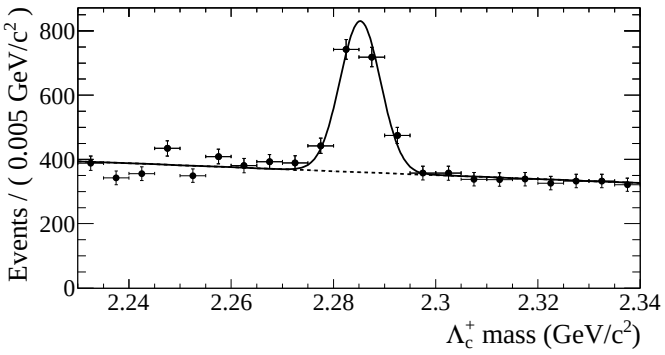

FIG. 3: Fit to the Λ_c^+ distribution for $\overline{B} \to \Lambda_c^+ X$. The data are shown as points with error bars, the overall fit as a solid line, and the combinatorial $B\overline{B}$ and continuum background as a dashed line.

Many systematic uncertainties approximately cancel in this ratio, such as those due to the Λ_c^+ and $B_{\rm tag}$ reconstruction efficiencies and the Λ_c^+ decay branching fractions. We categorize the remaining systematic uncertainties into those which directly affect the signal yield, and those which affect only the branching fraction ratio. The systematic uncertainties that have been considered are described below and summarized in Table II.

Systematic uncertainties in the signal yield are dominated by the peaking-background yield estimate. We estimate this by propagating the uncertainty in the $\overline{B} \to \Lambda_c^+ X$ branching fraction, and the Poisson error from the Monte Carlo statistics. We add in quadrature the effect of varying the lepton misidentification probabilities by 15% for both electrons and muons. To account for a possible bias in the fit technique, we perform ensembles of Monte Carlo experiments, in which events are generated according to the PDF shapes measured on data, varying the signal to background rate, and fitting for the signal as in the full analysis. The average difference between the fitted value of the yield and the Monte Carlo true value is taken as a systematic error, labeled "Fit bias" in table II.

TABLE I: Signal yields and reconstruction efficiencies for the $\overline{B} \to \Lambda_c^+ X \ell^- \overline{\nu}_\ell$, $\overline{B} \to \Lambda_c^+ X$, and $B/\overline{B} \to \Lambda_c^+ X$ decays with the corresponding statistical uncertainties.

Decay Mode	$N_{\rm data}$	ε ($\times 10^{-5}$)
$\overline{B} \to \Lambda_c^+ X e^- \overline{\nu}_e$	15.0 ± 6.8	1.98 ± 0.17
$\overline{B} \to \Lambda_c^+ X \mu^- \overline{\nu}_\mu$	-6.2 ± 6.3	1.04 ± 0.12
$\overline{B} \to \Lambda_c^+ X$	934 ± 55	3.09 ± 0.11
$B/\overline{B} \to \Lambda_c^+ X$	1386 ± 66	3.21 ± 0.12

Systematic uncertainties on the reconstruction efficiency ratio are dominated by the uncertainty in the signal model. This is estimated by comparing our nominal signal model with a pure phase space model, where the $\overline{B} \to \Lambda_c^+ X \ell^- \overline{\nu}_\ell$ decay occurs in one step, taking the full difference in the signal efficiency estimate compared to our nominal signal model as the systematic uncertainty. We estimate the effect of particle identification systematic uncertainties on the signal efficiency by varying the electron (muon) identification efficiency by 2% (3%) respectively. Because the event selection algorithms are slightly different in the semi-leptonic and inclusive samples, the $B_{\rm tag}$ and Λ_c^+ reconstruction efficiency ratio uncertainties do not exactly cancel. We evaluate the corresponding systematic uncertainty by reversing the order of the lepton and $B_{\rm tag}$ selection in signal Monte Carlo, and comparing the reconstruction efficiency with our standard selection order. We find the reversed selection order efficiency to be compatible with the standard selection order efficiency within the precision of our Monte Carlo statistics, and so we estimate the systematic uncertainty as the statistical error of the efficiency comparison.

As a cross-check of the signal model, we compare the measured shapes of the Λ_c^+ and electron momentum spectra in our semi-leptonic sample, assuming that the observed excess of events is due to semileptonic $\overline{B} \to \Lambda_c^+ X e^- \overline{\nu}_e$ decays, with those predicted by our nominal signal model. To reduce the impact of combinatorial background on this comparison, we subtract the spectra measured in the Λ_c^+ invariant mass sideband region, scaled to the signal region. We find a $\Delta\chi^2/\text{n.d.f.} < 1$ when comparing the histograms of these spectra, showing our model is consistent with the data.

TABLE II: Table of systematic uncertainties. The errors on the signal yield are shown in units of events, those on on the reconstruction efficiency ratio are shown in units of percent.

yield systematics (ev.)	$\ell = e$	$\ell = \mu$
Peaking background: MC statistics	1.0	1.4
Peaking background: $\mathcal{B}(\overline{B} \to \Lambda_c^+ X)$	1.6	4.7
Lepton miss-id rate	0.7	2.0
Fit bias	0.3	1.2
Total	2.0	5.4
efficiency ratio systematics (%)	$\ell = e$	$\ell = \mu$
Reco. efficiency statistics	8.4	11.4
Signal Model	11.3	35.9
Lepton id efficiency	1.1	2.7
Selection order	5.0	6.8
Total	15.0	38.4

We measure the following branching ratios:

$$\begin{aligned}
\frac{\mathcal{B}(\overline{B} \to \Lambda_c^+ X e^- \overline{\nu}_e)}{\mathcal{B}(\overline{B} \to \Lambda_c^+ X)} &= (2.5 \pm 1.1_{\rm stat.} \pm 0.6_{\rm syst.})\% \\
\frac{\mathcal{B}(\overline{B} \to \Lambda_c^+ X \mu^- \overline{\nu}_\mu)}{\mathcal{B}(\overline{B} \to \Lambda_c^+ X)} &= (-2.0 \pm 2.0_{\rm stat.} \pm 1.9_{\rm syst.})\% \\
\frac{\mathcal{B}(\overline{B} \to \Lambda_c^+ X \ell^- \overline{\nu}_\ell)}{\mathcal{B}(\overline{B} \to \Lambda_c^+ X)} &= (1.7 \pm 1.0_{\rm stat.} \pm 0.6_{\rm syst.})\%. \quad (3)
\end{aligned}$$

We find a signal significance $\mathcal{S} = 2.1$, including the signal yield systematic uncertainties, from the difference in the log likelihood between the nominal fit and a fit in which we fix the signal yield to zero. From scanning the likelihood values we estimate the 90% confidence level upper limit $\mathcal{B}(\overline{B} \to \Lambda_c^+ X \ell^- \overline{\nu}_\ell)/\mathcal{B}(\overline{B} \to \Lambda_c^+ X) < 3.5\%$. As a cross-check, we repeat the analysis without requiring charge-flavor correlation between the lepton and the charged $B_{\rm tag}$ and without correcting for mixing. After re-estimating backgrounds, we find consistent results as in Eq. 3, but with lower significance.

For a comparison with the CLEO result [4] in which the flavor of the semi-leptonic B was not determined, we repeat the analysis without requiring the charge-flavor correlation between the $B_{\rm tag}$ and the Λ_c^+ in the normalization mode. The yield for the normalization mode without requiring the charge-flavor correlation is shown in Tab. I. We obtain the branching fraction ratio

$$\frac{\mathcal{B}(\overline{B} \to \Lambda_c^+ X \ell^- \overline{\nu}_\ell)}{\mathcal{B}(B/\overline{B} \to \Lambda_c^+ X)} = (1.2 \pm 0.7_{\rm stat.} \pm 0.4_{\rm syst.})\% \quad (4)$$

with its corresponding 90% confidence level upper limit $\mathcal{B}(\overline{B} \to \Lambda_c^+ X \ell^- \overline{\nu}_\ell)/\mathcal{B}(B/\overline{B} \to \Lambda_c^+ X) < 2.5\%$, which improves the existing result.

In conclusion, we have presented a search for semi-leptonic B decays into the charmed baryon Λ_c^+. We obtain an improved upper limit with respect to previous measurements [2] on the relative branching fraction $\mathcal{B}(\overline{B} \to \Lambda_c^+ X \ell^- \overline{\nu}_\ell)/\mathcal{B}(\overline{B} \to \Lambda_c^+ X)$, which is found to be much smaller than the corresponding relative branching fraction for B decays into charmed mesons. Our result shows that the rate of baryonic semi-leptonic B

decay is too small to substantially contribute to the inclusive semi-leptonic B decay branching fraction.

We are grateful for the excellent luminosity and machine conditions provided by our PEP-II colleagues, and for the substantial dedicated effort from the computing organizations that support *BABAR*. The collaborating institutions wish to thank SLAC for its support and kind hospitality. This work is supported by DOE and NSF (USA), NSERC (Canada), CEA and CNRS-IN2P3 (France), BMBF and DFG (Germany), INFN (Italy), FOM (The Netherlands), NFR (Norway), MES (Russia), MEC (Spain), and STFC (United Kingdom). Individuals have received support from the Marie Curie EIF (European Union) and the A. P. Sloan Foundation.

* Now at Temple University, Philadelphia, Pennsylvania 19122, USA
† Also with Università di Perugia, Dipartimento di Fisica, Perugia, Italy
‡ Now at University of South Alabama, Mobile, Alabama 36688, USA
§ Also with Università di Sassari, Sassari, Italy

[1] The charge conjugate state is always implied unless stated otherwise.
[2] K. Nakamura *et al.* (Particle Data Group), J. Phys. G**37**, 075021 (2010).
[3] B. Aubert *et al.* (*BABAR* Collaboration), Phys. Rev. Lett. **100**, 151802 (2008).
[4] G. Bonvicini *et al.* (CLEO Collaboration), Phys. Rev. D **57**, 6604 (1998).
[5] B. Aubert *et al.* (*BABAR* Collab.), Nucl. Instrum. Methods A**479**, 1 (2002).
[6] S. Agostinelli *et al.*, Nucl. Instrum. Methods A**506**, 250 (2003).
[7] B. Aubert *et al.* (*BABAR* Collab.), Phys. Rev. Lett. **92**, 071802 (2004).
[8] T. Sjostrand, Comput. Phys. Commun. **82**, 74 (1994).
[9] J. L. Goity and W. Roberts, Phys. Rev. D**51**, 3459 (1995).
[10] W. D. Hulsbergen, Nucl. Instrum. Methods A**552**, 566 (2005).
[11] B. Aubert *et al.* (*BABAR* Collab.), Phys. Rev. D**69**, 111104 (2004).